Effect of Shocks on Mixing and Thrust in Over-expanded Nozzles

Swapneel Roy[1], Thanusha M.T[2], Rahul B.V[3], A.A. Khan[4]

[1, 2, 3] Aeronautical Society of India, 13-B, Indraprastha Estate, New Delhi, India

[4] Propulsion Division, CSIR - National Aerospace Laboratories, Bangalore. India

[1]swap.roy88@gmail.com; [2]thanushreya@yahoo.co.in; [3]rahulbv2047@yahoo.co.in; [4]ashfaque@nal.res.in

Abstract

The flow in the divergent part of a highly over-expanded nozzle suffers strong instability due to formation of shock waves which causes mixing enhancement in the flow and destabilizes the shear layer adjacent to it. The code FLUENT has been used to simulate the flow of two different viscous fluids (air and hydrogen) through five different Convergent-Divergent (C-D) nozzles of varying area ratio and exit angles. 2-D steady state RANS equation has been simulated for both inviscid and viscous flow. SSTKW (Shear Stress Transport k-ω) turbulence model has been invoked to capture the viscous flow phenomena efficiently. The converged solution shows basic viscous flow phenomenon like lambda shock for NPR≥1.32, asymmetric lambda shock for NPR≥1.40 and flow separation for NPR≥1.32. In addition, turbulent kinetic energy increases sharply with the shock and asymmetric flow separation. Separated flow reattaches at the smaller leg of the lambda shock. However, it continues to be separated till the exit at the larger leg side of the lambda shock for NPR≥1.65 (for nozzles with α_e>0°). Mixing efficiency at the exit of the nozzle rises with increase in NPR for NPR≤1.72. But this increase in mixing efficiency could not continue for higher NPRs. The thrust for computed viscous predictions decreases with NPR upto NPR=1.8 and then starts increasing. The computed results are generally in trends with the experiments as far as shock; in addition, aftershock and mixing are concerned.

Keywords

Lambda Shock; Asymmetry; Mixing; Turbulent Kinetic Energy; Thrust

Nomenclature

α = Half Nozzle Angle,

A, Y = Cross Sectional Area, Mass Fraction

P, T, ϱ = Pressure, Temperature, Density

M, U = Mach number, axial velocity

F = Actual nozzle thrust

F_i = Ideally expanded nozzle thrust

P_d = Normalized total pressure

NPR = Nozzle Pressure Ratio

γ = Specific heat ratio

Subscripts

i, e, a = inlet, exit, ambient

t = throat

u, l = upper, lower wall

h_2, O_2 = hydrogen, oxygen

mix = uniformly mixed

ac = actual

0 = total

Introduction

Flow separation in supersonic convergent-divergent nozzles has been the subject of numerous experimental and numerical studies in the past by Papamoschou et al. [2004, 2000], Xiao et al. [Jan. 2007], Craig A. Hunter [1998, 2004], Zill [2006] and Khan et al. Over-expanded conditions occur when the supersonic nozzle is operated at NPRs well below the design NPR, resulting in shock formation and flow separation. The 1-D inviscid theory fails to predict the complex flow structure.

For lower NPRs, a bowed normal shock appears in the divergent section of the nozzle. As the NPR is increased, the flow separates due to adverse pressure gradients and the shock bifurcates in the form of a lambda shape which consists of an incident shock, reflected shock, and Mach stem. The point of co-incidence of these shocks is known as triple point. The incident shock turns the flow away from the wall whereas the reflected shock tries to turn back the flow to the original direction. The flow behind the Mach stem is subsonic because of the normal shock. However, the flow behind the reflected shock is still supersonic. Papamoschou et al. [2004] explained that

the whole flow behind the lambda shock is divided into two regions separated by slip stream which originates from the triple point. The supersonic flow behind the reflected shock accelerates for a short distance because of expansion waves. The subsonic flow behind the Mach stem also accelerates because of the convergent divergent region formed due to the wavy slip stream. Papamoschou et al. [2004] also showed that the slip stream becomes supersonic at the position where it is intercepted by the expansion wave. Ultimately, the flow may experience another shock in the downstream known as aftershock to match the ambient pressure as shown in fig. 1. At higher NPRs, the flow separates asymmetrically, where one lambda foot is larger than the other. The asymmetric flow separation has been predicted by Xiao et al. [2007] for higher NPR (1.5<NPR<2.4) depending upon the initial flow field. For higher NPRs (NPR≥2), Craig A. Hunter [1998, 2004] analyzed that the separation is not a result of a stronger shock-wave/boundary-layer interaction, but it comes through the natural tendency of an over-expanded nozzle flow.

Chen et al. showed that the peak value of wall static pressure is associated with reattachment of flow. Over-expanded nozzles are characterized with unsteady shock induced separation. The unsteady nature of shock boundary interaction is explained by K.C. Muck et al., W.J. Baars et al. and Rahul et al.

Most of the earlier nozzle studies are focused on the prediction of mixing by studying the jet plume exiting the nozzle as explained by Papamoschou [2000], Zill [2006] and Xiao et al. [Jan. 2007, 2009]. In the study of co-axial flows, Papamoschou [2000] concluded that mixing enhancement was connected with the operation of C-D nozzle at NPRs well below the design value.

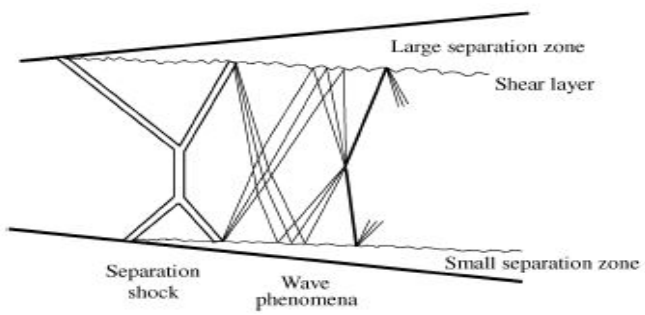

FIG. 1 SCHEMATIC DIAGRAM OF SHOCK STRUCTURE IN AN OVER-EXPANDED SUPERSONIC NOZZLE [HAMED ET AL].

Zill [2006] showed that the mixing enhancement is evident starting with nozzle pressure ratios as low as 1.40 and becomes dominant over a wide range of NPRs, typically between 1.60 and 2.50. Zill [2006] also showed that mixing enhancement is a function not only of NPR but also of local nozzle exit angle and area ratio. Xiao et al. [Jan. 2007] studied that, with increasing area ratio, the total pressure loss has been observed to increase due to large separation downstream of the shock, initiating mixing inside the nozzle.

Xiao et al. [Jan. 2007, 2009] observed that asymmetric flow separation resulted in significant increase in turbulent kinetic energy and with increasing area ratio, the peak level rises and moves towards the nozzle exit. Since over-expanded flow results in total pressure losses, it is important to predict the thrust loss and thrust performance of the nozzle. Papamoschou [2009] suggested that the thrust predictions (compared with inviscid predictions) for these type of nozzle flows would be inaccurate because of the non-uniformity of the flow at the exit. Asbury et al. showed that the off-design nozzle thrust coefficient could be improved by encouraging stable separation (with a passive porous cavity) and controlling the location and extent of that separation.

The present study concentrated on predicting mixing quantitatively inside the nozzle in the presence of shock formation and comparison was made between the numerical results and the earlier experimental values.

Computational Details

The computational domain and grid of five different C-D nozzles have been generated using GAMBIT. Nozzle1:- A_e/A_t=1.7, α_e=3.03°; Nozzle 2:- A_e/A_t=1.5, α_e=0.0°; Nozzle 3:- A_e/A_t=1.4, α_e=0.0°; Nozzle 4:- A_e/A_t=1.5, α_e=2.12°; Nozzle 5:- A_e/A_t=1.5, α_{eu}=4.33°, $A_{el}=A_{tl}$. Nozzle 5 is asymmetric about centreline. The geometry has been chosen from the published work of Zill [2006]. The computational domain at the inlet is shown in fig. 2 indicating air and hydrogen inlets. 2-D steady state RANS equation has been simulated using boundary layer grid based on y^+=1. Pressure based grid adaptation has been invoked to capture the shock accurately. Simulations have been done on both inviscid and viscous flows in all the five nozzles. Viscous flow results are shown in greater detail. SSTKW (Shear Stress Transport k-ω) turbulence model

was chosen based on the previous experience. Xiao et al. [Jan 2007, 2009] and Hamed et al. have also shown that SST model gives the best overall agreement with the experimental results in case of over-expanded nozzles. Computations have been started with the initial grid size (quadrilateral grid) in the range of 11360 to 11440 in different nozzles, but with grid adaptation, the final solutions were obtained on grids that had 1.75 to 3 times than the original number of cells. The inlet boundary conditions consisted of P_0=3.5x10^{5}N/m^2 and T_0=300K. The exit static pressure was varied to obtain different NPRs ranging from 1.19 to 2.36.

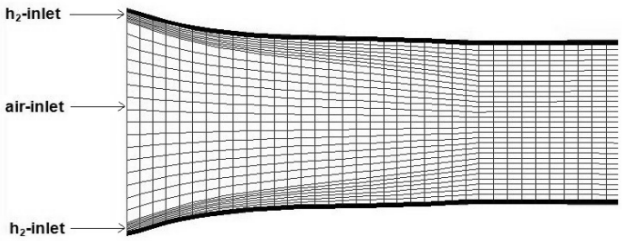

FIG. 2 COMPUTATIONAL DOMAIN AT THE INLET

Results and Discussion

Computations were done on five different C-D nozzles at different NPRs to predict the influence of area ratio, nozzle symmetry and exit angle on the flow features, shock structure, mixing efficiency and thrust performance. The results obtained were generally in agreement with the experimental results.

Flow Pattern and Shock Structure

The converged viscous solutions predicted tilted (normal) shock for NPR≤1.28, symmetric lambda shock for 1.32≤NPR≤1.37, asymmetric lambda shock for NPR≥1.40 and also captured aftershocks for higher NPRs. Fig. 3 shows Mach number contour of Nozzle1 at NPR=1.92, where asymmetric lambda shock and after shock(s) can be seen. The size of the Mach stem reduces with increase in NPR creating large separation zones at the larger lambda foot side for asymmetric shocks. Flow separation takes place for NPR≥1.32. The separated flow reattaches at the smaller leg side of the lambda shock for all NPRs, whereas, for nozzles with α_e>0°, flow continues to be separated for NPR≥1.65. Fig. 4 shows the plot of x-wall shear stress for NPR=1.92 (nozzle1) indicating flow separation and reattachment. The basic predicted flow features (i.e. tilted shock, symmetric and asymmetric lambda shock, aftershock and flow separation) have been obtained by Zill [2006] in the experiments too.

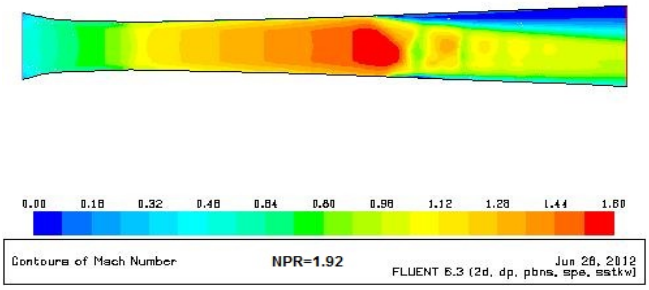

FIG. 3 MACH NUMBER CONTOUR FOR NPR=1.92, NOZZLE1

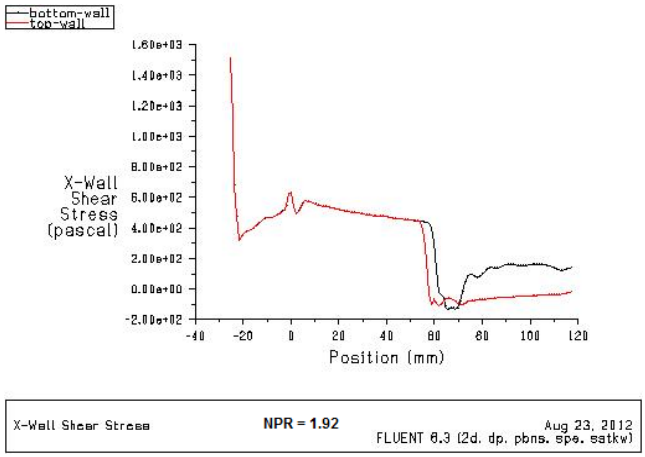

FIG. 4 PLOT OF X-WALL SHEAR STRESS FOR NPR=1.92, NOZZLE1

Mixing Efficiency

Mixing efficiency has been calculated based on the equation given by Liu et al.

$$\eta_m = \frac{\int \rho U \varphi dy}{\int \rho Y_{h_{2_{mix}}} U dy}, \varphi = \begin{cases} Y_{h_{2_{ac}}}, Y_{h_{2_{ac}}} \le Y_{h_{2_{mix}}} \\ \dfrac{Y_{o_{2_{ac}}}}{\left(\dfrac{Y_{o_{2_{mix}}}}{Y_{h_{2_{mix}}}}\right)}, Y_{h_{2_{ac}}} > Y_{h_{2_{mix}}} \end{cases}$$

The mass fraction of hydrogen (Y_{h2ac}) near the walls is greater than the uniformly mixed value of hydrogen (Y_{h2mix}) which makes the mixing efficiency greater than one where Y_{h2ac}>Y_{h2mix}. Hence, at points where Y_{h2ac}>Y_{h2mix}, the mixing efficiency is based on the mass fraction of oxygen. Mixing efficiency (η_m) at the exit of the nozzle rises with increase in NPRs for NPR≤1.72. It has been found to be maximum in the range of 1.72≤NPR≤1.92 for nozzles with α_e>0°, 1.6≤NPR≤1.89 for nozzles with α_e=0° and 1.6≤NPR≤1.81 for geometrically asymmetric nozzle.

Fig. 5 shows η_m at different NPRs for all the nozzles. In the experiment by Zill [2006], mixing was dominant for 1.6≤NPR≤2.5 for A_e/A_t>1.6. For similar exit area

ratio, asymmetric nozzle has higher η_m for NPR≤1.44, whereas for higher NPRs, η_m is higher in symmetric nozzles as shown in Table I which also shows the percentage increase in η_m for consecutive NPRs. It is observed that the percentage increase in η_m is generally higher at transition from tilted shock to symmetric lambda shock and symmetric to asymmetric lambda shock. η_m adds with increase in exit area ratio, which is due to the formation of large separation zones creating large eddies at the larger lambda foot side of the wall as explained by Zill [2006]. For same area ratio, η_m is higher for nozzles with α_e>0° till NPR≤1.44 after which, η_m is higher for nozzles with α_e=0° as shown in Table II.

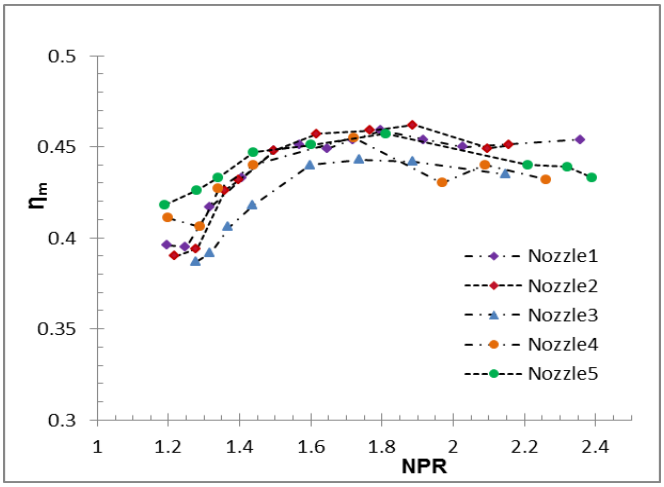

FIG. 5 MIXING EFFICIENCY PLOT AT THE OUTLET FOR DIFFERENT NOZZLES

TABLE I COMPARISON OF MIXING EFFICIENCY FOR SYMMETRIC AND ASYMMETRIC NOZZLES AT A_e/A_t=1.50

Nozzle2 (symmetric)			Nozzle5 (asymmetric)		
NPR	η_m	% increase	NPR	η_m	% increase
1.22	0.39	-	1.19	0.418	-
1.28	0.394	1.03	1.28	0.426	1.91
1.36	0.426	8.12	1.34	0.433	1.64
1.4	0.432	1.41	1.44	0.447	3.23
1.5	0.448	3.70	1.6	0.451	0.89
1.62	0.457	2.01	1.81	0.457	1.33
1.77	0.459	0.44	2	0.443	-3.06
1.89	0.462	0.65	2.21	0.44	-0.68
2.1	0.449	-2.81	2.32	0.439	-0.23
2.16	0.451	0.45	2.39	0.433	-1.37

TABLE II COMPARISON OF MIXING EFFICIENCY FOR A_e >0° AND A_e =0° AT A_e/A_t=1.5

Nozzle4 (α_e>0°)			Nozzle2 (α_e=0°)		
NPR	η_m	% increase	NPR	η_m	% increase
1.2	0.411	-	1.22	0.39	-
1.29	0.406	-1.22	1.28	0.394	1.03
1.34	0.427	5.17	1.36	0.426	8.12
1.44	0.44	3.04	1.4	0.432	1.41
1.72	0.455	3.41	1.5	0.448	3.70
1.97	0.43	-5.49	1.77	0.459	2.46
2.09	0.44	2.33	1.89	0.462	0.65
2.26	0.432	-1.82	2.16	0.451	-2.38

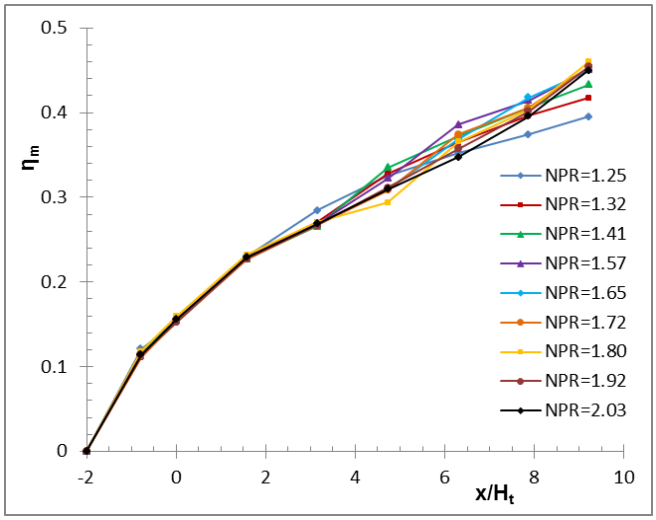

FIG. 6 MIXING EFFICIENCY PLOT FOR NOZZLE1

Fig. 6 shows mixing efficiency in different locations at varying NPRs for Nozzle1. The coincidence of the curves in the initial region of the nozzle (convergent part and initial part of the divergent section) before the shock at different NPRs clearly indicates the effect of shock on mixing enhancement.

Mixing efficiency can also be quantified in terms of axial total pressure decay. Fig. 7 shows the plot of P_d vs. x/H_t for nozzle1 at different NPRs. It is evident from the plot that mixing is dominant at NPRs between 1.57 and 1.92 which matches well with the results shown in Fig. 5. Fig. 8 compares total pressure decay for different nozzles at NPR close to 1.60. It can be seen that mixing increases with area ratio. Similarly for the same NPR and area ratio, mixing is higher for nozzles with α_e=0°, which again matches well with the results shown in Fig. 5.

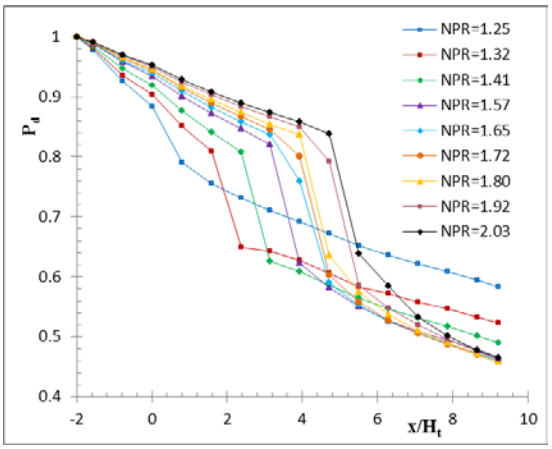

FIG. 7 PLOT OF TOTAL PRESSURE DECAY FOR NOZZLE1

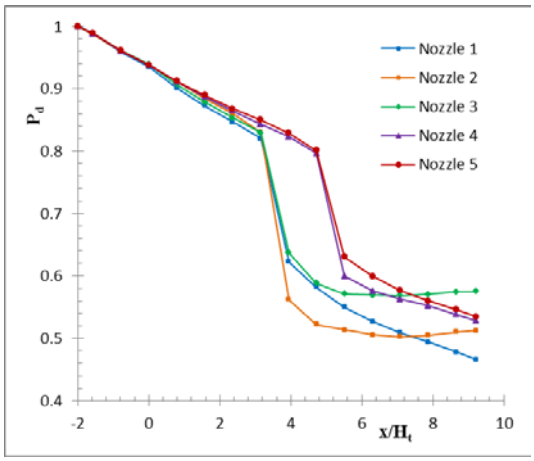

FIG. 8 PLOT OF TOTAL PRESSURE DECAY FOR DIFFERENT NOZZLES (NOZZLE1-NPR=1.57, NOZZLE2-NPR=1.62, NOZZLE3-NPR=1.60, NOZZLE4-NPR=1.60, NOZZLE5-NPR=1.60)

Turbulent Kinetic Energy

The turbulent kinetic energy increases with the shock and further increases with asymmetric flow separation as it destabilizes the flow. Fig. 9 shows the turbulent kinetic energy for different NPRs at the line passing through Mach stem for Nozzle1.

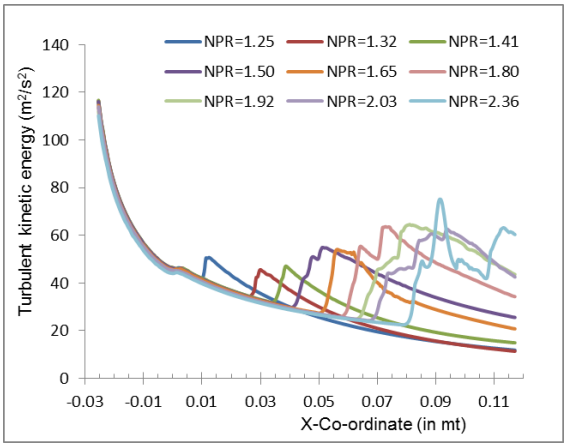

FIG. 9 TURBULENT KINETIC ENERGY PLOT FOR DIFFERENT NPR, NOZZLE1

Thrust Performance

The thrust co-efficient is the ratio of actual nozzle thrust (F) to the ideally expanded nozzle thrust (F_i). The thrust calculations are based on the general formula given below.

$$\frac{F}{P_{0_i} A_t} = \frac{A_e}{A_t}\left[\frac{\gamma M_e^{\,2}}{NPR}\left(\frac{P_e}{P_a}\right) + \frac{1}{NPR}\left(\frac{P_e}{P_a} - 1\right)\right]$$

Fig. 10 shows the plot of thrust co-efficient vs. NPR for five different nozzles. The thrust coefficient is considerably less at NPRs well below the design point. The theoretical values of thrust co-efficient have been obtained based on one dimensional inviscid theory to compare the computational results (inviscid and viscous). The measured thrust coefficient for viscous flow is found to be less than theoretical predictions at all NPRs due to higher total pressure losses resulted from the occurrence of lambda shock and aftershocks. However, the thrust coefficient starts increasing for NPR>1.8, where fully detached stable separations have been found. Furthermore, it could be the result of reduction in the number of aftershocks at higher NPRs, which reduces total pressure losses. The inviscid computational result (shown only for NPRs where shock is in the diverging section of the nozzle) matches well with the theoretical prediction.

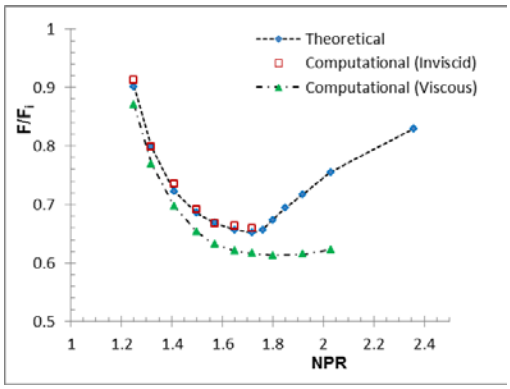

FIG. 10(A) THRUST CO-EFFICIENT FOR NOZZLE1 AT DIFFERENT NPR

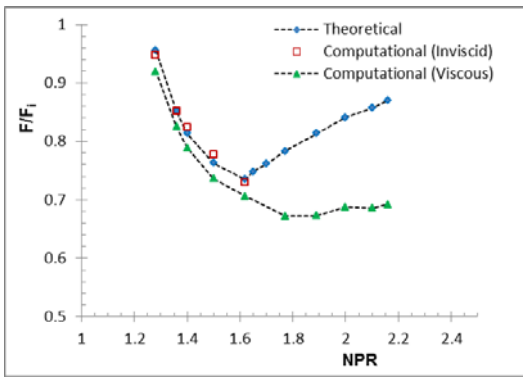

FIG. 10(B) THRUST CO-EFFICIENT FOR NOZZLE2 AT DIFFERENT NPR

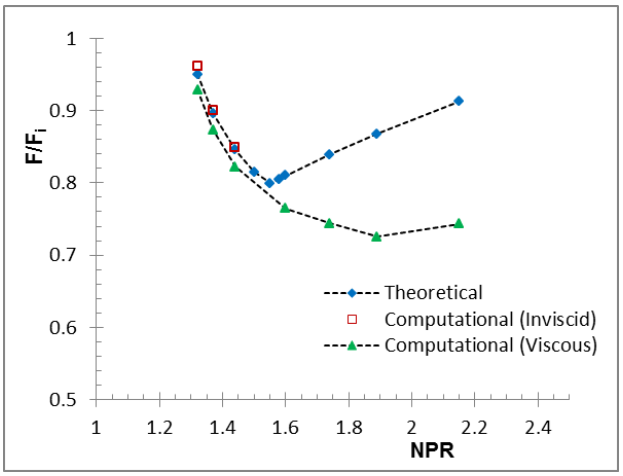

FIG. 10(C) THRUST CO-EFFICIENT FOR NOZZLE3 AT DIFFERENT NPR

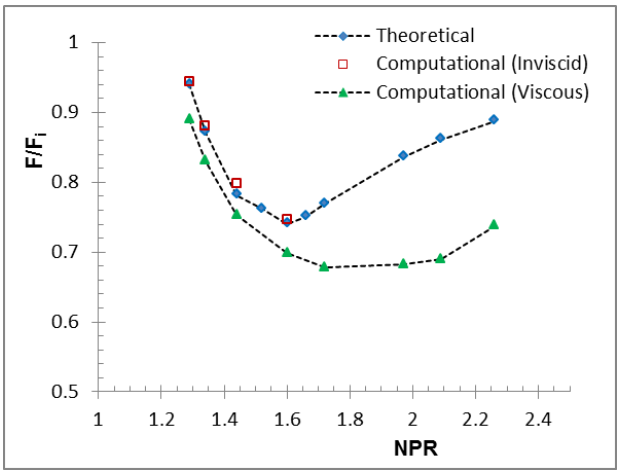

FIG. 10(D) THRUST CO-EFFICIENT FOR NOZZLE4 AT DIFFERENT NPR

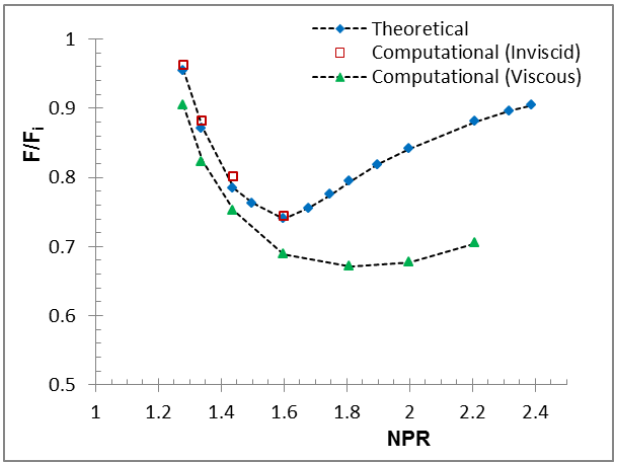

FIG. 10(E) THRUST CO-EFFICIENT FOR NOZZLE5 AT DIFFERENT NPRS

Fig. 11 shows the thrust co-efficient comparison for viscous analysis in different nozzles. The thrust coefficient decreases with increase in exit area ratio for the same NPR. It also shows that the thrust coefficient is mostly a function of exit area ratio and doesn't vary much with the change in geometry of the nozzle. Nozzle2, nozzle4 and nozzle5 have the same exit area ratio with different geometry but the variation in thrust co-efficient is minimal for the same NPR.

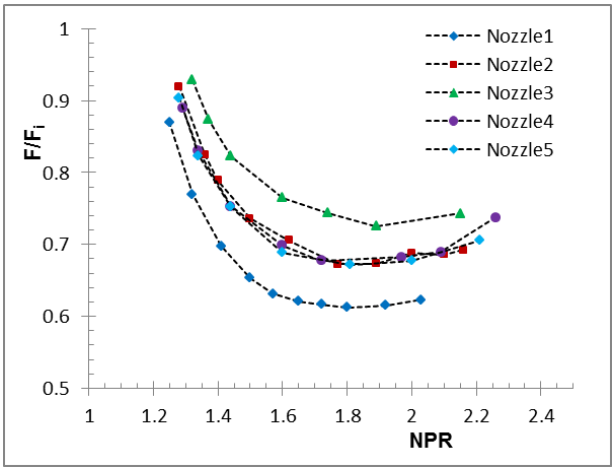

FIG. 11 COMPARISON OF THRUST CO-EFFICIENT FOR COMPUTATIONAL VISCOUS ANALYSIS IN DIFFERENT NOZZLES

Conclusions

The simulated viscous flows have captured asymmetric lambda shock for NPR≥1.40 and aftershock(s) for higher NPRs. Separated flow (i.e. for NPR≥1.32) reattaches at the smaller leg side of the lambda shock for all NPRs, whereas, for nozzles with α_e>0°, flow continues to be separated for NPR≥1.65.

Mixing efficiency is dominant in the range 1.6≤NPR≤1.92 for all nozzles. Formation of asymmetric lambda shocks have enhanced mixing for higher NPRs. In addition, η_m rises with increase in exit area ratio due to formation of larger separation zones creating larger eddies. For same exit area ratio, η_m is higher in symmetric nozzles for NPR≥1.44. Additionally, for NPR≥1.44, η_m is higher for nozzles with α_e=0° as compared to nozzles with α_e>0° for the same exit area ratio. The total pressure decay plot also confirmed the above data.

Turbulent kinetic energy increases with asymmetric flow separation, destabilizing the flow. The computational thrust co-efficient has been found to be less than corresponding theoretical values, which decreases with increase in NPR till NPR=1.8 and then starts increasing due to fully detached stable separation. Thrust co-efficient decreases with increase in exit area ratio too. The exit angle and asymmetry in geometry does not affect the thrust co-efficient significantly.

ACKNOWLEDGMENT

The authors would like to thank Director, CSIR - NAL to allow us to do this work, Head, Propulsion Division for his continuous encouragement during this work, Dr. Venkat S. Iyengar and Mr. Sathiyamoorthy K. (Scientists, Propulsion Division, CSIR - NAL) for their valuable suggestions and comments and CSIR - CMMACS, Bangalore for providing their computing facilities for this work.

REFERENCES

Asbury, Scott C., Gunther, Christopher L. and Hunter, Craig A. "A Passive Cavity Concept for Improving the Off-Design Performance of fixed-Geometry Exhaust nozzles", AIAA Paper 1996-2541, 1996.

Baars, W.J., Tinney, C.E., Ruf, J. H., Brown, A. M. and McDaniels D.M. " On the Unsteadiness associated with Shock-Induced Separation in Over-expanded Rocket Nozzles", 46th AIAA/ASME/SAE/ASEE Joint Propulsion Conference and Exhibit, 2010-6728, 2010.

Chen, C. L., Chakravarthy, S. L. and Hung, C. M."Numerical investigation of separated Nozzle Flows", AIAA Journal Vol.32, 1836-1843, 1994.

Hamed, A. and Vogiatzis, C. "Overexpanded Two-Dimensional Convergent-Divergent Nozzle Flow Simulations, Assessment of Turbulence Models", Journal of Propulsion and Power, Vol.13, No.3, 444-445, 1997.

Hunter, Craig A. "Experimental Investigation of Separated Nozzle Flows", AIAA Journal 20(3), 527-532, 2004.

Hunter, Craig A. "Experimental, Theoretical and Computational Investigation of Separated Nozzle Flows", AIAA Paper 1998-3107, 1998.

Khan, A.A. and Shembharkar, T.R. "Viscous Flow analysis in a Convergent-Divergent Nozzle", Proceedings of International Conference on Aerospace Science and Technology, INCAST 2008 004, 2008.

Liu, Hui and Xing, Yuming. "Unsteady Flow and the Mixing Efficiency in Transverse Jets", 978-1-61284-459-6/11, IEEE 2011.

Muck, K.C., Dussage, Jean-Paul and Bogdonoff S.M. "Structure of the Wall Pressure fluctuations in a shock-Induced Separated Turbulent Flow", AIAA Paper 1985-0179, 1985.

Papamoschou, D and Zill, Andreas. "Fundamental investigation of supersonic nozzle flow separation", AIAA Paper 2004-1111, 2004.

Papamoschou, Dimitri. "Mixing Enhancement Using Axial Flow", AIAA Paper 2000-0093.

Rahul B.V., Roy, Swapneel, Thanusha M.T., and Khan A.A. "Unsteady Computation of Over-Expanded Flow in a Convergent Divergent Nozzle", International Conference on Computing, Communications, systems and Aeronautics (ICCCSA-2012), 30-31 March, 2012.

Xiao, Q, Tsai, H.M. and Papamoschou, D. "Numerical investigation of supersonic nozzle flow separation", AIAA Journal, 45(3), 532-541, 2007.

Xiao, Q., Tsai, H.M. and Papamoschou, D. "Numerical Study of Jet Plume Instability from an Over-expanded Nozzle", 45th AIAA Aerospace Sciences Meeting and Exhibit, 8-11 January 2007, Reno, Nevada.

Xiao, Q., Tsai, H.M., Papamoschou, D. and Johnson, Andrew. "Experimental and Numerical Study of Jet Mixing from a Shock-Containing Nozzle", Journal of Propulsion and Power, Vol.25, No.3, May-June 2009.

Zill, Andreas. "Flow Separation in Rectangular Over-expanded Supersonic Nozzles", AIAA Paper 2006-17, 2006.